13214–13227 *Nucleic Acids Research, 2014, Vol. 42, No. 21* *Published online 11 November 2014*
doi: 10.1093/nar/gku1148

Double-stranded DNA-dependent ATPase Irc3p is directly involved in mitochondrial genome maintenance

Tiina Sedman, Ilja Gaidutšik, Karin Villemson, YingJian Hou and Juhan Sedman*

Institute of Molecular and Cell Biology, University of Tartu, Riia 23b, Tartu 51010, Estonia

Received May 09, 2014; Revised October 13, 2014; Accepted October 28, 2014

ABSTRACT

Nucleic acid-dependent ATPases are involved in nearly all aspects of DNA and RNA metabolism. Previous studies have described a number of mitochondrial helicases. However, double-stranded DNA-dependent ATPases, including translocases or enzymes remodeling DNA-protein complexes, have not been identified in mitochondria of the yeast *Saccharomyces cerevisae*. Here, we demonstrate that Irc3p is a mitochondrial double-stranded DNA-dependent ATPase of the Superfamily II. In contrast to the other mitochondrial Superfamily II enzymes Mss116p, Suv3p and Mrh4p, which are RNA helicases, Irc3p has a direct role in mitochondrial DNA (mtDNA) maintenance. Specific Irc3p-dependent mtDNA metabolic intermediates can be detected, including high levels of double-stranded DNA breaks that accumulate in *irc3Δ* mutants. *irc3Δ*-related topology changes in *rho-* mtDNA can be reversed by the deletion of mitochondrial RNA polymerase RPO41, suggesting that Irc3p counterbalances adverse effects of transcription on mitochondrial genome stability.

INTRODUCTION

Mitochondria are dynamic eukaryotic organelles required for energy production and for a number of catabolic and anabolic pathways. Most mitochondrial proteins are encoded by the nuclear genome and are imported into mitochondria via a post-translational mechanism (1). However, a small number of essential respiratory chain peptides (8 in yeast) are encoded by mitochondrial DNA (mtDNA) (2). As a result, defective maintenance of the mitochondrial genome contributes to mitochondrial dysfunction, which in humans can lead to metabolic diseases, cancer, neurological disorders and contribute to aging (3–5).

Yeast mtDNA is replicated by the single-subunit DNA polymerase γ (2,6). While a large number of genes affecting the stability of the mitochondrial genome in the yeast *Saccharomyces cerevisiae* have been identified (7), the functions of many accessory proteins required for mtDNA maintenance have only partially been established. *In vivo* studies of mtDNA metabolism have been conducted in two rather different mitochondrial genetic backgrounds, using either wild-type (wt) (*rho*+) or respiratory deficient *rho*− strains. Relatively little is known about the replication process and intermediates of the *wt rho*+ mitochondrial genome of *S. cerevisiae*, which is about 85 kb long (2,6). In most cases, respiratory inactive *rho*− mutants have been studied, where a short (often less than 1 kb) non-functional mtDNA fragment is retained and amplified as tandem repeats (8). Preferential transmission of specific hypersuppressive (HS) *rho*− mitochondrial genomes in genetic crosses, similarity between the *ori* sequences found in HS mutants and the heavy-strand origin in mammalian mtDNA, and biochemical evidence on RNA-DNA hybrid molecules have generated a model of transcript mediated initiation of DNA synthesis at the *ori* elements of yeast mtDNA (9). According to this model, mitochondrial RNA polymerase Rpo41p functions also as a primase during the initiation of mtDNA synthesis (10–13). It should be noted that several protein factors are not required for *rho*− genome maintenance, but essential for the wt *rho*+ mitochondrial genome, indicating that the inheritance mechanisms of the *rho*+ genome are more complex compared to *rho*− mutants (14–16). Mitochondrial protein synthesis is essential for the stability of the *rho*+ mtDNA (17). Therefore, mutants that affect mitochondrial transcription, splicing or ribosomal RNA maturation also destabilize the *rho*+ mtDNA, further complicating functional assignment of proteins involved in mitochondrial nucleic acid metabolism.

Defective mitochondrial gene expression and the accumulation of mitochondrial genome mutations can damage the respiratory chain complexes. This in turn can impact the stability of the nuclear genome through mechanisms that could involve the generation of reactive oxygen species and the synthesis of iron sulfur clusters that requires proper mitochondrial membrane potential (18,19). Previously, a genome-wide screen for increased levels of spontaneous Rad52 foci was carried out in *S. cerevisiae* to iden-

*To whom correspondence should be addressed. Tel: +372 7375837; Fax: +372 7420286; Email: juhan.sedman@ut.ee

tify mutants that affect formation and processing of double-stranded breaks in nuclear DNA (20). A group of genes identified in the screen had known or predicted functions in mitochondria, supporting the idea that mitochondrial dysfunction can be harmful for the integrity of nuclear DNA or activate a damage response signaling pathway. In addition to previously characterized genes, the screen also identified 22 novel IRC genes (IRC, Increased Recombination Centers) with no known biological function. This group of genes included IRC3, which had been predicted to encode a mitochondrial protein in a large-scale green fluorescent protein (GFP)-fusion protein localization study (21).

In silico analysis suggests that Irc3p belongs to a large group of proteins, historically known as the superfamily II (SFII) of helicases (22–24). SFII proteins possess RNA helicase, DNA helicase or nucleic-acid translocase activities (22). Yeast mitochondria contain three previously characterized SFII enzymes, Mss116p, Suv3p and Mhr4, all involved in RNA metabolism. Mss116p, a general RNA chaperone, is required for intron splicing and translational activation (25–29). Suv3p is a key component of the mitochondrial RNA degradasome, has a role in splicing and possibly in mtDNA maintenance (30–33). Mhr4p is involved in mitochondrial ribosome biogenesis (34,35). The enzymatic activities and the biochemical functions of Irc3p are unknown.

Here, we confirm that Irc3p is targeted to mitochondrial matrix and possesses double-stranded DNA (dsDNA)-dependent adenosine triphosphatase (ATPase) activity. Our analysis of mutant yeast strains reveals that in contrast to the other mitochondrial SFII family proteins, Irc3p is directly involved in mtDNA metabolism. Furthermore, our data suggest that Irc3p could stimulate recombination-dependent double-stranded break repair and could have a role in the stable maintenance of actively transcribed regions in the yeast mitochondrial genome.

MATERIALS AND METHODS

Yeast strains, plasmids and media

Yeast strains used in this study were isogenic with W303–1A or W303–1B and are described in the Supplementary Table S1. Yeast knockout strains were made by replacing the corresponding open reading frame (ORF) with the KAN or the HPH cassette via homologous recombination. The oligonucleotides used for generation of the knockout strains and Irc3p-HA are enlisted in the Supplementary Table S2.

pRS315-IRC3 contains the IRC3 ORF, 400 bp upstream of the ATG codon and 432 bp downstream of the stop codon, cloned between BamHI and SacI sites of the vector. pRS315-IRC3Δ15 and pRS315-IRC3Δ28 were constructed by deleting the first 15 or 28 codons of the IRC3 ORF and adding the sequence of BamHI site GGATCC and the ATG codon to the remaining part of IRC3 ORF. IRC Δ28-NCIT1 was generated by inserting the first 114 codons of Cit1p preprotein into BamHI site of pRS315-IRC3Δ28.

Standard yeast media YPD, YPG and SD were prepared as described previously (36). Solid media contained 2% agar. 0.1% 5-FOA (5-fluoroorotic acid) in SD was used for the plasmid shuffling assay.

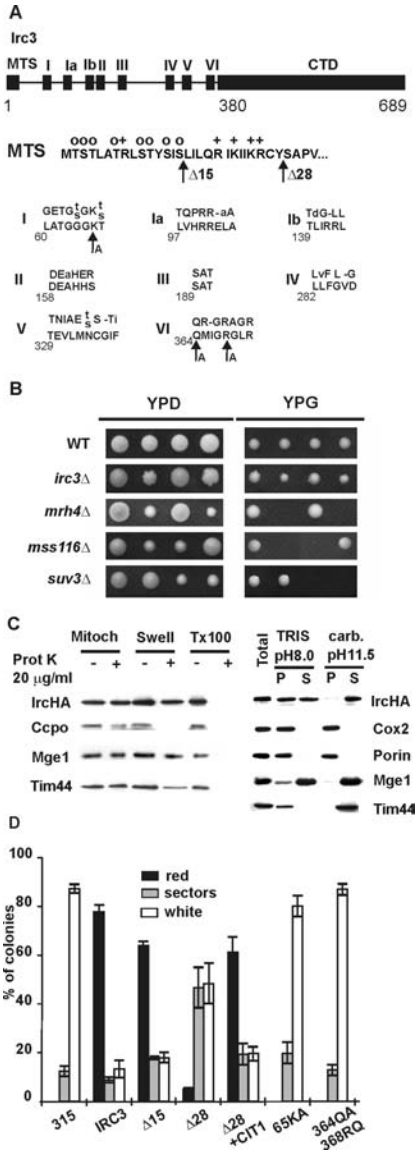

Figure 1. Irc3p is a mitochondrial matrix protein. (A) Schematic representation of Irc3p showing the positions of helicase motifs I–VI compared to DEAH family protein consensus, MTS and CTD. O, hydroxylated aminoacids; +, positively charged aminoacids. The arrows indicate the deletions used to verify the matrix targeting signal and the conserved residues mutated in the motifs I and VI to obtain ATPase mutants. (B) Sporulation of W303 wt diploid yeast strain and heterozygous mutants of the mitochondrial SFII family on media containing fermentable (YPD) or non-fermentable (YPG) carbon sources at 30°C. (C) Submitochondrial localization of Irc3p. Left, intact mitochondria, mitoplasts or Triton-X100 lysed mitochondria were treated with proteinase K and subjected to immunoblot analysis with the indicated antibodies. Right, mitochondria were disrupted with sonication and extracted with Tris pH8 or Na_2CO_3 pH11.5, the unsoluble (P) and soluble (S) fractions were analyzed by immunoblotting with the indicated antibodies. Ccpo, intermembrane space protein; Mge1p, matrix protein, weakly associated with the inner membrane; Tim44p, peripheral inner membrane protein; Cox2p, integral inner membrane protein; Porin, outer membrane protein. (D) 5-FOA-based shuffling assay of Irc3 mutants. Yeast cells with the wt IRC3 on the URA3 plasmid pRS316 and the indicated irc3 mutant on the LEU2 plasmid pRS315 were plated on 5-FOA, -Leu SC media and incubated for 3 days at 30°C, followed by 4 days at RT. The colonies were counted as white (no respiration), red (respiratory active) or sectored (mixed, containing >5% cells with different color). Error bars on all figures represent the standard deviation of three independent assays or cultures unless stated otherwise.

Fractionation of mitochondria and immunoblots

Preparation of mitochondria for biochemical fractionation and immunoblotting was performed as described previously (14).

ATPase assay

The ATPase activity of Irc3p was analyzed in 30 mM Tris 7.5, 7 mM Mg, 1 mM DTT, 0.1 mg/ml bovine serum albumin, 0.1 mM adenosine triphosphate (ATP) at 30°C essentially as previously described (37). Different polynucleotide cofactors were used at 7.5 μM (nucleotides) if not stated otherwise.

Determination of petite formation and analysis of mtDNA loss

Ten milliliter yeast overnight cultures were grown in YPG to select for respiratory-competent cells and used to inoculate YPD cultures (100 ml) in 500 ml flasks to an $OD_{600} = 0.02$. The YPD cultures were diluted again to $OD_{600} = 0.04$ before reaching density $OD_{600} = 0.8$. The fraction of mutant petite cells was determined immediately after inoculation of the YPD cultures and at later timepoints as indicated on the Figure 2B. Petite frequency was determined by plating triplicates onto YPD and YPG plates. Total cellular DNA was prepared from 10–20 ml yeast culture according to the previously described method (14). The dynamics of mtDNA loss was analyzed by quantitative polymerase chain reaction (qPCR). A total of 20 ng of total yeast DNA was used for amplification reactions using mitochondrial *COX2* gene and nuclear *HMI1* gene as targets. Amplifications were performed in triplicates and used to calculate the relative ratio of mtDNA to nuclear DNA. The primers of the amplification reactions are described in Supplementary Table S2.

Analysis of mtDNA topology on 2D agarose gels

DNA was purified from isolated mitochondria as previously described (38). A total of 10 μg of mtDNA was treated with the indicated restriction enzymes according to manufacturer's protocols (Fermentas). Upon treatment, the reaction was stopped by the addition of 6× gel loading buffer and neutral 2D-agarose gel-electrophoresis was carried out. DNA fragments of sizes between 2.5 and 4.5 kb were separated in 0.5% first dimension gels at 0.9 V/cm at room temperature (RT) for 18 h and in 1.2% second dimension gels containing 300 ng/ml of ethidium bromide at 6 V/cm and 4°C for 6–7 h. rho–a1184 mtDNA was separated in 0.4% first dimension gels at 0.9 V/cm at RT for 16 h. DraI digested rho-DNA was separated in 1.5% second dimension gels run for 6 h, 5V/cm. Undigested rho-DNA was run in 1% second dimension gels for 4 h, 5V/cm.

DNA transfer to positively charged nylon membranes (Applichem) and Southern blotting in modified Church buffer was performed as described previously (38). Specific PCR probes and end-labeled oligonucleotides used for the hybridization of DNA blots are described in Supplementary Table S3. The filters were exposed to Storage Phosphor Screens (GE Healthcare), signals detected with a Typhoon Trio Phosphor Imager (GE Healthcare) and quan-

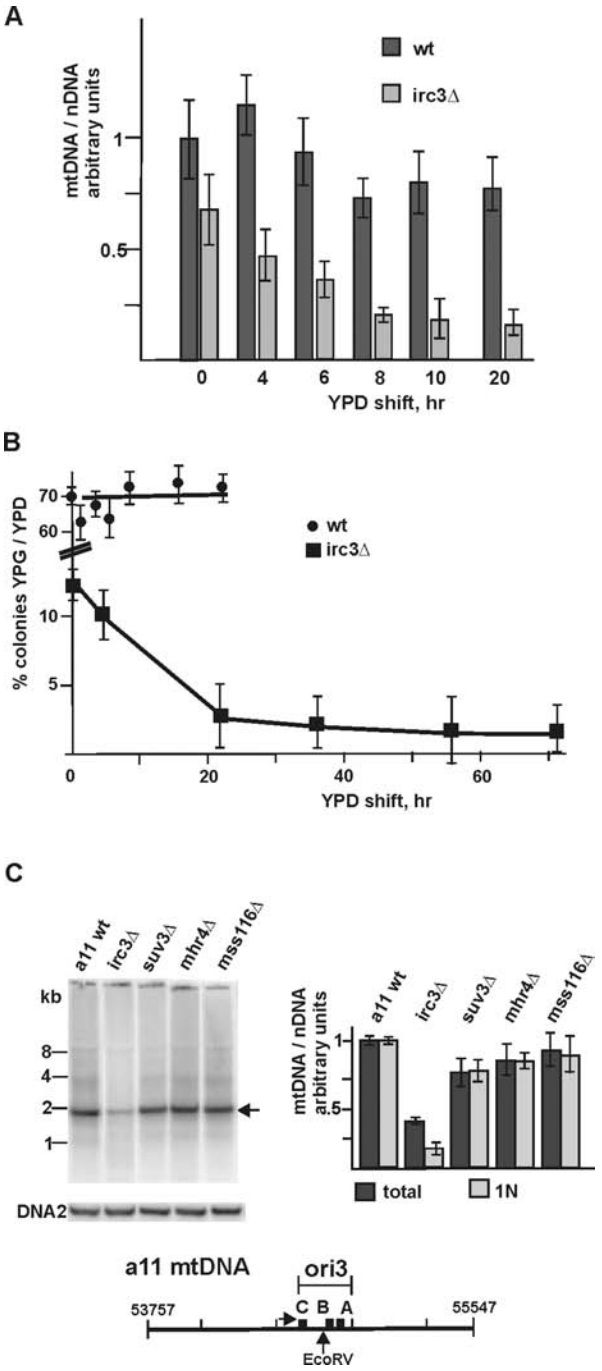

Figure 2. Loss of respiratory competence and instability of the mitochondrial genome in the *irc3*Δ yeast mutant. (A) wt and *irc3*Δ cultures were shifted from glycerol medium to glucose and relative mtDNA copy number was measured at the indicated time points with qPCR. mtDNA/nuclear DNA ratio 1 corresponds to the ratio in wt strain at 0-timepoint. (B) Respiratory competence of wt and *irc3*Δ yeast cells was analyzed in the same cultures by plating onto agar medium containing glucose (YPD) or glycerol (YPG). (C) Comparision of a11 rho− mtDNA digested with EcoRV in different SFII family disruption strains. Left, representative mtDNA Southern blot of a11 strain with the nuclear DNA standard (DNA2). Right, quantification of relative mtDNA copy numbers. Lower panel, schematic representation of a11 mtDNA. mtDNA/nuclear DNA ratio 1 corresponds to the ratio in wt strain. Total corresponds to the integrated signal of all mtDNA. 1N is the signal that corresponds to the specific unit size fragment. Error bars here represent the standard deviation of six independent biological replicas.

tifications carried out with ImageQuant TL software (GE Healthcare).

RESULTS

Irc3p is a DExH/D-box protein localized to the mitochondrial matrix and is required for the respiratory competence of yeast cells

The *IRC3* gene in *S. cerevisae* encodes a putative DExH/D-box protein of SFII helicases. The sequence of Irc3p reveals core structural motifs I–VI, conserved among nucleoside triphosphate (NTP)-dependent nucleic acid translocases and a C-terminal domain (CTD) of unknown function (Figure 1A). The first 28 N-terminal residues of Irc3p form a putative mitochondrial targeting signal (MTS), which is in agreement with a high-throughput localization study of GFP-fusion proteins that predicted a mitochondrial localization for Irc3p (21). To understand the biochemical function of Irc3p, we generated heterozygous knockout strains of *IRC3* and of three previously characterized mitochondrial SFII enzymes—*MSS116*, *MHR4* and *SUV3*. The *irc3Δ/IRC3* heterozygote formed four viable spores on media containing a non-fermentable carbon source. However, the two *irc3Δ* spores of 12 analyzed tetrads always displayed a significant growth defect compared to the *IRC3* spores (Figure 1B). In contrast, sporulation of *mss116Δ/MSS116*, *mhr4Δ/MHR4* or *suv3Δ/SUV3* heterozygotes yielded only two viable spores on glycerol (Figure 1B). These three mitochondrial SF2 family enzymes are required for mitochondrial gene expression and are therefore essential for growth on non-fermentable carbon sources as previously reported (34,39,40). On YPD agar, the *irc3*Δ spores formed colonies with a characteristic ragged edge, indicating that the colonies frequently produce sectors of respiratory-deficient cells. The growth defect of *irc3*Δ cells was also observed in liquid YPG medium. The centromeric plasmid pRS315-IRC3 containing the wt *IRC3* gene restored wt growth rate on glucose containing agar plates to some but not all transformed colonies of the W303a *irc3*Δ strain. Rapidly growing cells contained the wt mitochondrial genome while slowly growing clones were *rho*− (data not shown). These findings suggested that Irc3p could have a mitochondrial function with possible role in mtDNA maintenance but the protein is not essential for mitochondrial gene expression.

To confirm that Irc3p is targeted to mitochondria, we tagged the protein with the HA epitope at the C-terminus and analyzed the intracellular localization of the protein by biochemical fractionation (Figure 1C). Irc3p-HA complemented the phenotypic defects of the *irc3*Δ strain (Supplementary Figure S1). Irc3p-HA was found to cofractionate with mitochondria and the protein was resistant to proteinase K treatment of purified mitochondria. Hypotonic swelling of mitochondria and selective rupture of the outer membrane did not expose Irc3p-HA for proteinase K degradation, demonstrating that Irc3p is localized in the matrix compartment of mitochondria (Figure 1C, left panel). Sonication experiments were next performed to analyze the association of Irc3p with the mitochondrial membranes (Figure 1C, right panel). Isolated mitochondria were disrupted by sonication in a hypotonic buffer solution and the resulting suspension of mitochondrial membrane fragments was extracted with Na_2CO_3 pH11.5 to separate the fraction of peripherial membrane proteins. In contrast to integral membrane marker protein Cox2p or matrix protein Mge1, Irc3p was distributed between the soluble and insoluble fractions after sonication. Extraction of membranes with Na_2CO_3 pH11.5 completely solubilized Irc3p, indicating that Irc3p is not an integral membrane protein. However, we cannot exclude the possibility that a subfraction of the protein is associated with the inner membrane (Figure 1C). The fractionation pattern of Irc3p-HA did not change when mitochondria were isolated from respiratory-deficient *rho*− yeast cells containing defective mtDNA or from *rho0* yeast cells, which do not contain mtDNA at all (Supplementary Figure S2). A similar fractionation profile was previously obtained for another yeast mitochondrial SFI DNA helicase—Hmi1p, involved in mitochondrial genome maintenance (14).

The N-terminus of Irc3p contains basic and hydroxylated residues characteristic for a MTS (Figure 1A). *In silico* analysis predicts a mitochondrial matrix pre-protein peptidase MPP cleavage site between the residues 28 and 29 (...$KRCY_{28}$::S_{29}APV...) (41). The predicted cleavage site also corresponds to the mature Irc3p N-terminus according to mass spectrometric analysis of peptides obtained from partially purified Irc3p-HA (data not shown). To confirm that the N-terminal targeting sequence is essential for Irc3p function, we generated two N-terminal deletion mutants, *IRC3*–15Δ and *IRC3*–28Δ, which lack 15 or 28 N-terminal residues, respectively, and checked their ability to complement *wt IRC3* in a plasmid shuffling assay (Figure 1D). In this assay, the W303 *irc3Δ* strain with *wt IRC3* on pRS316-*IRC3* was transformed with pRS315-*irc3*, containing a mutant *irc3*. The cells were plated out on SC-Leu agar with 0.1% 5-FOA to counterselect the pRS316-*IRC3*. Due to the *ade2* mutation in the W303 yeast strain, respiration-competent cells accumulate a red pigment while respiratory-deficient petite cells are white. In our shuffling assay, 90% of colonies with pRS315 (negative control) were white and 10% contained red sectors (Figure 1D). More than 80% of colonies with pRS315-wt-*IRC3* (positive control) were red. Approximately 65% of colonies with pRS315-*irc3*(NΔ15) were red and less than <5% of colonies with pRS315-*irc3*(NΔ28) were red (Figure 1D). This indicated that the *irc3*(NΔ15) mutant had lost some activity and the *irc3*(NΔ28) mutant was almost completely inactive, confirming that the 28 N-terminal amino acid residues are required for Irc3p activity. Importantly, the functionality of Irc3p was restored when the native Irc3p targeting sequence (the residues 1–28) was replaced with the targeting peptide from the mitochondrial citrate synthase Cit1p (N-terminal 85 residues of the pre-protein) (75% red colonies). Therefore, the main function of the N-terminal peptide of Irc3p is to target the protein to mitochondria (Figure 1D). Finally, we used the plasmid shuffling assay to test the mutants of the conserved helicase motifs I and VI in Irc3p (Figure 1A). K65 of motif I is predicted to coordinate the β-phosphate of ATP and a K-A substitution is expected to abolish ATPase activity of the protein (42). Similarly, the Q364 and the R368 of motif VI are predicted to be important for ATPase activity as mutations in similar positions in the DEAH protein

Prp22 drastically reduced ATPase activity (43). Both Irc3p-65KA and Irc3p-364QA/368RA mutants were unable to complement the loss of wt *IRC3* in the shuffling assay (Figure 1D). We concluded that the ATPase activity is essential for the functionality of the Irc3 protein and the findings confirm that Irc3 is a mitochondrial matrix protein.

Irc3p is required for the stability of mitochondrial genome maintenance

The growth characteristics of W303a *irc3Δ* cells suggested that *irc3Δ* mutants frequently lose the functional *rho*+ mitochondrial genome. To analyze the stability of wt mtDNA in the W303 *irc3Δ* yeast strain, we measured the ratio of mtDNA to nuclear DNA (relative mtDNA copy number) during yeast growth under non-selective conditions by qPCR. Relative mtDNA copy number was measured by amplification with mitochondrial gene *COX2*-specific primers and nuclear gene *HMI1*-specific primers (Figure 2A). Respiratory-proficient yeast cells were pre-selected on glycerol and then released into glucose-containing medium where exponential growth was maintained for several days. Following the transfer to glucose medium, the mitochondrial genome copy number in *irc3 Δ* cells rapidly declined with the most drastic drop occurring during the first 8 h of growth. In *wt* yeast cells, only a small decrease in the relative copy number of mtDNA was observed (Figure 2A). In the mutant strain similar decline in mtDNA relative copy number was observed also with mitochondrial *COX3*- or *ATP6*-specific primers (Supplementary Figure S3). In addition to mtDNA copy number analysis, respiratory competence of yeast cells was analyzed by comparing viability of yeast cells on YPD and YPG plates (Figure 2B). A loss of respiratory competence essentially followed the decline of relative mtDNA copy number. Note that at timepoint zero a significantly smaller fraction (15%) of mutant W303 *irc3Δ* cells formed colonies on YPG plates compared to the 70% of *wt* W303 cells. The fraction of respiratory-competent W303 cells did not change significantly during cultivation in YPD. In contrast, the fraction of respiratory competent *irc3Δ* cells declined rapidly during the first 24 h after shift. Interestingly, a small number of *irc3Δ* cells retained respiratory competence even after 6 days of cultivation in YPD (Figure 2B). These data indicated that *irc3Δ* mutants slowly lose their functional mitochondrial genome and therefore the data were consistent with the idea that Irc3p is a mtDNA maintenance factor. However, a similar growth defect could also be an indirect result from gradual loss of mitochondrial gene expression in *irc3Δ* cells. Therefore, we next tested whether Irc3p also affects the copy number and the repeat stability of *rho*− mitochondrial genomes, which do not require transcription for their maintenance. Here, we used the *rho*− strain a11, isogenic with W303–1a, where a 1.79-kb mtDNA fragment with an active *ori3* is maintained (Figure 2C). The genes encoding *IRC3*, *MSS116*, *MHR4* or *SUV3* were disrupted in the a11 strain. Next, total cellular DNA was isolated from multiple independent colonies, digested with EcoRV, which cuts once in the 1.79 kb a11 repeat and quantified by Southern blots (Figure 2C). Quantification of a11-specific signals in comparison to the nuclear *DNA2* gene-specific signals revealed that the disruption of *IRC3* leads to more than 2-fold decrease in mtDNA levels compared to the parental a11 strain. In contrast, disruption of *SUV3*, *MHR4* or *MSS116* had little effect on mtDNA copy number in a11. Furthermore, the specific 1.79 kb fragment constituted a smaller fraction of the total mtDNA signal in *irc3Δ* strain compared to wt strain and the other mutants. We estimated that the specific signal corresponding to the 1.79-kb EcoRV fragment in a11 *irc3Δ* was ∼5–6 times weaker compared to the a11 *wt* and *suv3*, *mhr4* or *mss116* knockout strains. The a11 *rho*− mutant does not encode mitoribosome RNAs or tRNAs essential for the mitochondrial protein synthesis machinery. Thus, the effect of Irc3p could not be mediated by changes in mitochondrial gene expression and it is likely that Irc3p has a direct role in both *rho*+ and *rho*− mtDNA metabolism.

Specific double-stranded mtDNA breaks in the W303 *irc3Δ* mutant strain

To understand the nature of mtDNA fragmentation in more detail we analyzed the topology of DNA metabolic intermediates in both *rho*+ and *rho*− strains by 2D neutral agarose gel-electrophoresis (2D NAGE) that separates linear molecules and more complex species of the same mass. First, three different regions FI–FIII of the *rho*+ mitochondrial genome of the yeast *S. cerevisiae* were analyzed (Figure 3A, Supplementary Table S3). FI is a 1.9-kb EcoRV fragment that contains *tRNAMet* gene, a non0coding AT rich region and the 5′ half of the COX2 ORF. FII is a 2.5-kb EcoRI-StyI fragment that contains the active *ori 5*. The *ori* elements contain GC-rich boxes A, B and C; the boxes A and B can form a palindrome (11). Active *ori* elements in the yeast mitochondrial genome are associated with a non-anucleotide promoter and are believed to be related to transcription-driven initiation of DNA replication. FIII is a 2.3-kb ApaI fragment that contains the inactive *ori 6*. Inactive *ori* elements are similar to active *ori* elements but are not associated with a promoter. A substantial part of each fragment represents non-coding mtDNA, which is generally AT-rich but contains GC blocks as indicated in Figure 3A.

mtDNA was isolated from exponentially growing yeast cultures and digested with the indicated restriction enzymes. Different isoforms of mtDNA were next separated by NAGE according to their mass in the first dimension (D) and according to their mass and shape in the second D (Figure 3B). The 2D gels of *S. cerevisiae* mtDNA resolve dsDNA (Figure 3B, 'DS') and ssDNA molecules that form distinctive arcs (Figure 3B, 'SS'). Regular non-replicating dsDNA forms a 1N spot on the dsDNA arc (Figure 3B, '1N'). The characteristic Y arc (Figure 3B, 'Y') is generated by passing replication forks; the molecules comprising four-stranded structures, such as Holliday junctions, generate the almost vertical X-arc (Figure 3B, 'X'). A substantial fraction of yeast mtDNA molecules are not resolved into separate spots or arcs but form a highly heterogeneous, S1 nuclease sensitive blurred cloud that extends to the original gel well (Figure 3B, 'CL'). The Y-arc, the X-arc and the CL-molecules were detected in mtDNA isolated from both the *wt* yeast strain W303 and from the W303 *irc3Δ* mutant, as illustrated for the fragment FI (Figure 3C). These mtDNA isoforms are similar to the species described in the related

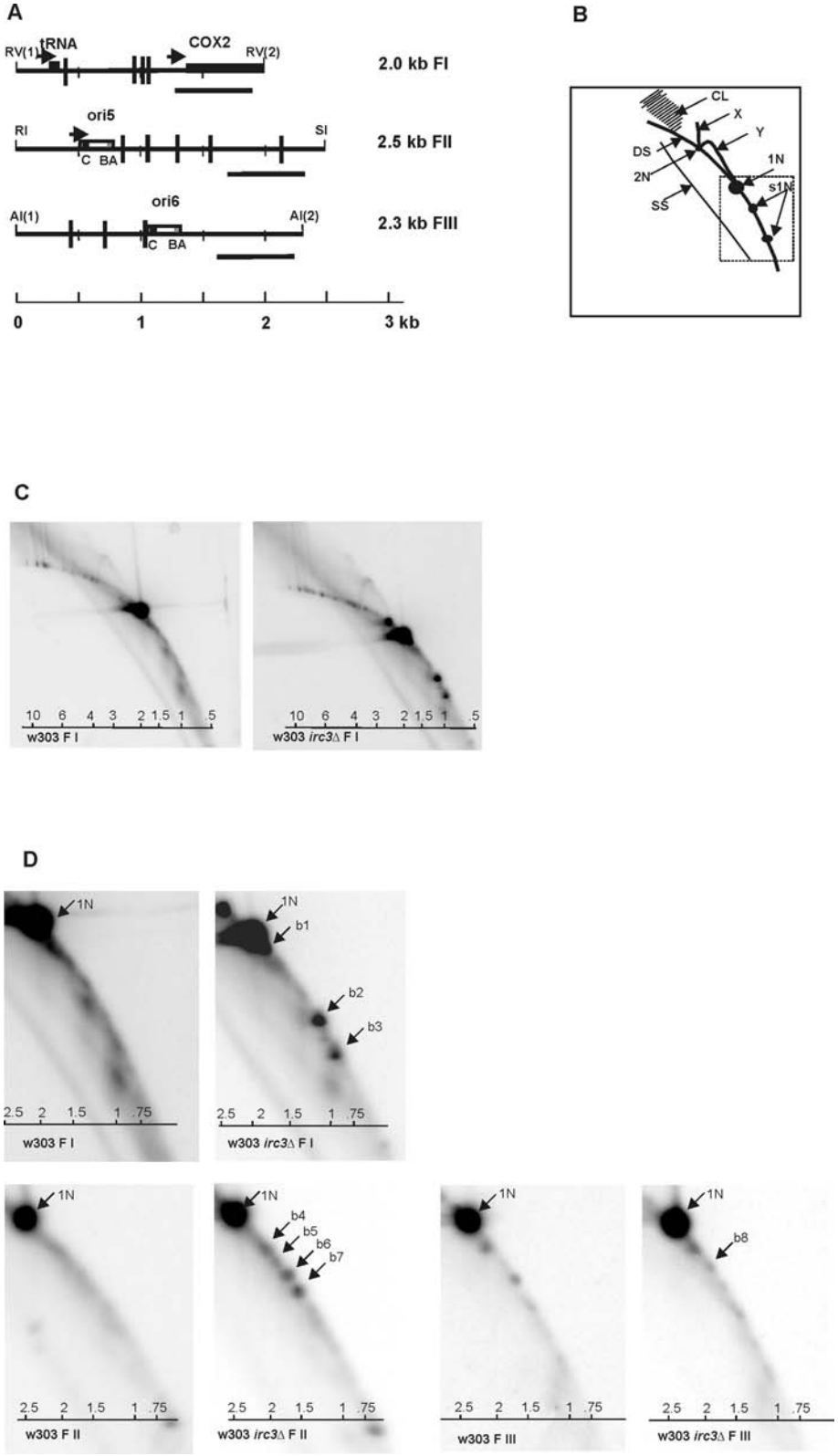

Figure 3. Double-stranded breaks or DNA-free ends accumulate at the GC-rich elements of transcribed regions of the wt *rho*+ mitochondrial genome in Δ*irc3* mutant. (A) Schematic representation of the analyzed restriction fragments of the *rho*+ mitochondrial genome. *COX2* and *tRNAMet* genes are indicated as black bars, *ori* elements as open bars with the C box at the beginning and the AB palindrome at the end of the *ori*. The vertical black bars indicate the positions of GC-rich clusters. The promoter elements are indicated by arrows. RV, EcoRV; RI, EcoRI; SI, StyI; AI, ApaI. Black bar below the fragment shows the probe used in the 2D NAGE analysis. (B) Schematic representation of 2D images. CL, complex branched molecules; X, X-arc; Y, Y-arc; DS, dsDNA; SS, ssDNA; s1N, smaller than 1N fragments. The rectangle indicates the approximate area of images on Figure 3D. (C) 2D NAGE analysis of the fragment FI. (D) 2D NAGE analysis of the fragments FI–FIII in the sub-1N regions. b1–b8 indicate spots on the dsDNA arc that are significantly stronger in the *irc3*Δ strain compared to the *wt* yeast.

yeast *C. albicans* (38). Notably, smaller than 1N (sub-1N) dsDNA species (Figure 3B, S1N) were detected in the yeast mtDNA (Figure 3C). Sub-1N regions of the three analyzed mtDNA fragments FI–FIII are shown on Figure 3D. A comparison of mtDNA isolated from the *wt* and the mutant yeast strains revealed additional distinctive spots on the dsDNA arc of the *irc3Δ* mutant indicated as b1–b8, which represent specific double-stranded breaks or free ends in the fragments (Figure 3D, Supplementary Figure S3). The intensity of hybridization signals in the spots b2 and b4 of the COX2 region was ∼5–8% of the regular 1N fragment signal and the signals of the spots b4–b7 in the ori5 region were 2–4% of the 1N signal.

In FI, the size of b2 and b3 (∼1.1 and 0.9 kb) corresponded to double-stranded breaks at the region of prominent GC clusters in the middle of the fragment FI. Similarly, the size of *irc3Δ*-specific novel spots in other fragments mostly correlated with the positions of GC clusters (Supplementary Figure S4).

Interestingly, active transcription appears to be another factor that stimulates the formation of dsDNA breaks. FII contains the *ori5*, which is actively transcribed and which displayed four *irc3Δ*-specific fragments b4–b7 close to the conserved ori structure. The size of b4 corresponded to a break at the box C of the active *ori5* and the size of b5 to a break near the A-B box palindrome of *ori5*. b6 and b7 breaks mapped further downstream of boxA.

However, in FIII the *ori6* is inactivated by an additional GC cluster insertion in the non-anucleotide promoter element. In this fragment only one fragment b8 that corresponded to a break at the GC cluster G14 was the only slightly enhanced spot in the *irc3Δ* mutant. No *irc3Δ*-specific breaks were mapped to the conserved *ori6* region. Therefore, transcription stimulates DNA fragmentation at the conserved *ori* elements of the *wt* mitochondrial genome. Interestingly, according to a recent analysis of the yeast mitochondrial transcriptome, the non-coding region in FI is transcribed in the opposite direction of *COX2* (44); furthermore, b1 in the same fragment mapped to a break either in the beginning of *COX2* or *tRNAMet* gene.

We conclude that in the absence of Irc3p, dsDNA breaks accumulate in yeast *rho*+ mtDNA. In the fragments FI and FII, prominent Irc3-dependent DNA breaks were associated with transcribed structural genes or active *ori* sequences and with GC-rich clusters. The data are in line with the idea that Irc3p is directly involved in mtDNA metabolism and could play a specific role in the transcribed regions of mtDNA.

Irc3p is *directly* involved in *rho*− mtDNA metabolism

In contrast to the *wt* mitochondrial genome, *rho*− mtDNA is maintained in the absence of gene expression in the organelle. Proteins that function exclusively in specific steps of mitochondrial gene expression, such as transcription, RNA maturation or protein biosynthesis, should therefore not influence the metabolism of *rho*− mtDNA. Here, we present our analysis of the HS a1184 *rho*− mt genome with a 1.2-kb repeat that contains active (transcribed) *ori2*, a partial inactive *ori7* and AT-rich spacers (Figure 4A).

The intact *rho*− mtDNA can be separated into linear double-stranded (DS), circular (C) and complex branched molecules (CL) as well as single-stranded DNA (ssDNA) species (SS) on 2D NAGE gels, schematically presented in Figure 4B. dsDNA concatemers of *rho*− mtDNA are believed to be a product of rolling-circle-type replication (45,46) and the circular molecules a result of intramolecular recombination (47). ssDNA molecules correspond to the non-transcribed strand ((10), our unpublished observations). If Irc3p was an RNA helicase with a sole function in mitochondrial gene expression, no Irc3p-dependent changes in *rho*− mtDNA metabolism would be expected. However, double-stranded concatemeric DNA molecules in the a1184 *irc3Δ* strain were significantly shorter compared to the *wt* a1184 strain, indicating that the synthesis of concatemeric *rho*− mtDNA by rolling-circle replication is inhibited in the absence of Irc3p (Figure 4C). The level of circular DNA molecules was significantly reduced and large circular molecules ($N > 3$) were virtually absent in the a1184 *irc3Δ* strain, which could reflect inhibition of recombination in the mutant. Finally, the population of ssDNA molecules was significantly shorter and reduced in the *irc3Δ* strain. To verify that the defects are Irc3p specific, we also analyzed the topology of intact mtDNA in *suv3Δ*, *mss116Δ* and *mrh4Δ* disruption strains in the a1184 background and found that the distribution of different mtDNA isoforms in these mutants is similar to the parental strain a1184 (Figure 4C). The latter result was expected for SFII enzymes involved in mitochondrial gene expression. We observed slight but reproducible decrease in the size of concatemeric double-stranded molecules in the a1184 *suv3Δ* strain (Figure 4C) and, interestingly, Suv3p has recently been reported to have an additional function in mtDNA maintenance (33).

a1184 mtDNA was also analyzed after treatment with DraI that cuts once in the a1184 1.2 kb DNA repeat at the promoter element next to the *ori2* C box (Figure 4A). Similarly to the *wt rho*+ mtDNA, the Y-arc (Figure 4B, 'Y') and the X-arc (Figure 4B, 'X') were detected in a1184 DNA, but also a number of additional complex arc structures running slower than the X-structure and that are characteristic for *rho*− genomic DNA (Figure 4D). DraI digested *rho*− DNA also displayed an arc of ssDNA (Figure 4B, 'SS'), mtDNA intermediates running between ssDNA and dsDNA arcs and complex unresolved molecules (Figure 4B, 'CL'). The specific X and Y arcs and more complex arc structures were much weaker in a1184 *irc3Δ*, and in contrast, the complex unresolved molecules ('CL' on Figure 4B) were more dominant in the mutant. This indicated that regular intermediates consisting of double-stranded branched DNA molecules are relatively rare in mitochondria of the *irc3Δ* strain. Notably, the arc of dsDNA was stronger and several distinctive <1N spots corresponding to specific dsDNA breaks were detected in the mtDNA of the a1184 *irc3Δ* strain (Figure 4D, s1, s3, s4). The size of s1 corresponds to a double-stranded break at the conserved C box of *ori2*; s3 corresponds to a break near the boxes B and A of *ori2* and s4 to a similar break near the boxes B and A of *ori7* (Figure 4A). Similar breakpoints at the conserved box A (b4) and near the boxes B and A (b5) of the actively transcribed *ori5* were detected in the *wt* mtDNA fragment

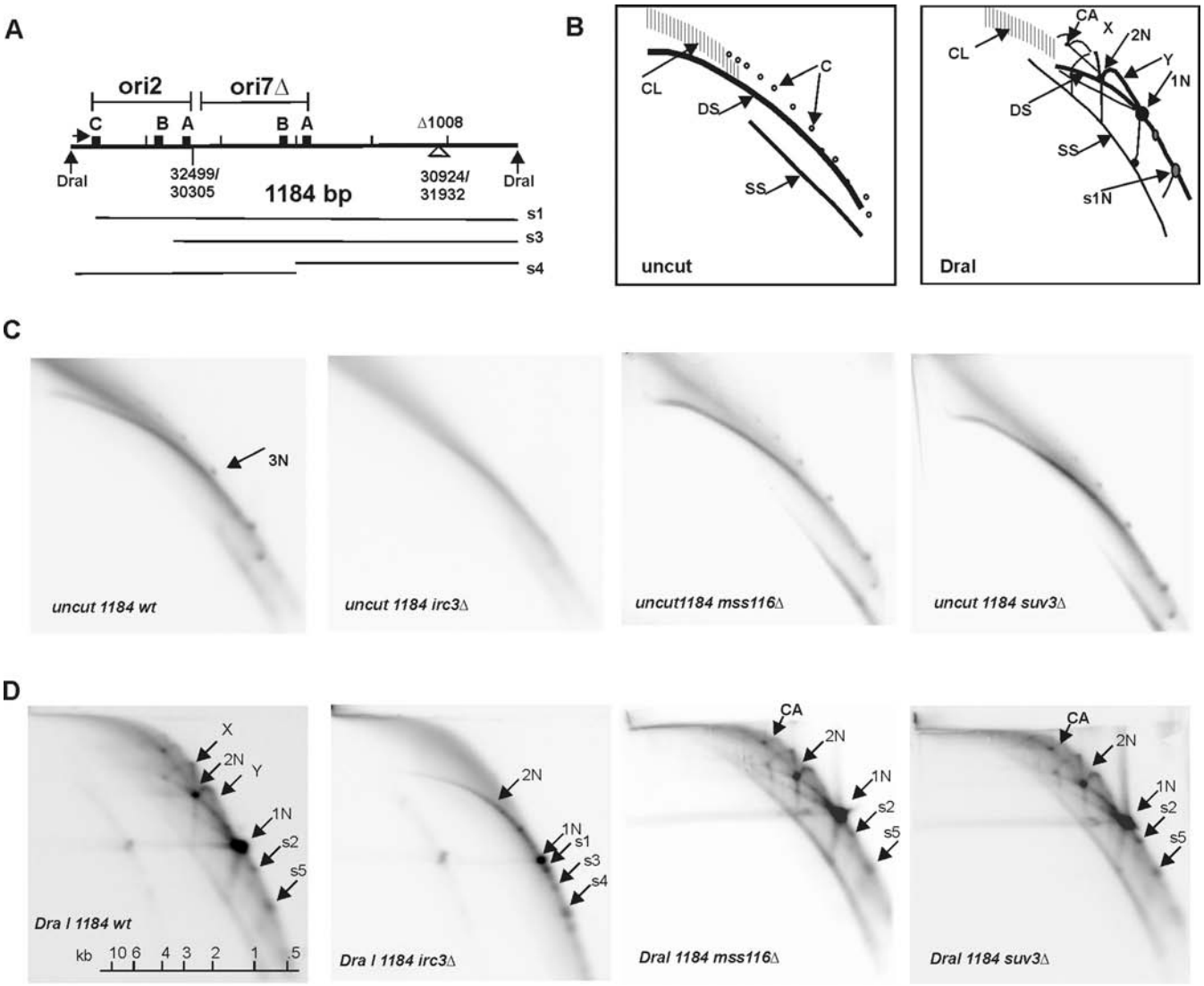

Figure 4. Deletion of *IRC3* results in the loss of recombination-dependent structures and accumulation of dsDNA breaks in *rho*− mitochondrial genome. (A) Schematic representation of the a1184 repeat. s1, s3 and s4 correspond to the *irc3*Δ-dependent fragments indicated in D. (B) Schematic representations of 2D NAGE gels of uncut and DraI digested *rho*− DNA preparations. (C) 2D NAGE analysis of undigested a1184 *rho*− mtDNA isolated from the wt and SFII family ATPase mutants. (D) 2D NAGE analysis of DraI digested a1184 *rho*− mtDNA isolated from the wt and SFII family ATPase mutants. s1, s3 and s3 are *irc3*Δ specific, s2 and s5 are present in all strains. All blots were probed with a ^{32}P labeled probe that covers the full length of the repeat.

FII of the W303 *irc3Δ* strain but not in the fragment FIII containing the inactive *ori 6* (Figure 3D). We next analyzed DraI digested mtDNA of the a1184 *MSS11* or *SUV3* disruption strains and found that deletion of SF II mitochondrial RNA helicases did not diminish the signals of double-stranded branched intermediates of a1184 mtDNA (the X and the Y arc). Furthermore, no significant accumulation of *irc3Δ*-specific fragments s1, s3 and s4 was detected in these mutants (Figure 4D). This again underlines the distinctive role of Irc3p in mtDNA metabolism. We conclude that the disruption of *IRC3* leads to the loss characteristic intermediates of DNA metabolism in *rho*− yeast strains and that similarly to the *wt rho*+ strain, these changes are accompanied with the accumulation of double-stranded breaks in yeast mtDNA.

Irc3p is a dsDNA-dependent ATPase

According to *in silico* predictions, Irc3p is a member of the SFII ATP-dependent nucleic acid translocases and helicases. The growth characteristics of the *irc3*Δ W303 yeast strain (Figure 1) suggested that in contrast to the three other mitochondrial SFII enzymes, Irc3p does not have an essential role in mitochondrial gene expression and must possess distinctive biochemical activities directly required for mtDNA maintenance. Furthermore, the analysis of *rho*− yeast strains suggested that Irc3p has a direct role of mtDNA metabolism. To understand the biochemical functions of Irc3p we overexpressed the protein in the pGEX-4T1-based bacterial expression system (GE Healthcare Life Sciences) and purified the protein by a combination of affinity chromatography and ion-exchange chromatography as described in Supplementary Materials and Methods and

Figure 5A. We first analyzed different natural yeast mitochondrial nucleic acid cofactors for the stimulation of Irc3p ATPase activity (Figure 5B). Total mitochondrial nucleic acid preparations efficiently stimulated Irc3p ATPase activity. The estimated k_{cat} value of the ATP hydrolysis reaction of the Irc3 protein is ~4 s^{-1} in the presence of mitochondrial nucleic acid as a cofactor at 30°C, which is in the typical range for SFII enzymes (48). mtDNA had a similar stimulatory effect as the total mitochondrial nucleic acid preparation, whereas mitochondrial RNA showed almost no stimulatory activity. We next tested several heterologous DNA and RNA cofactors (Figure 5C). The RNA cofactors (phage MS2 RNA and ribosomal 23S rRNA of *Escherichia coli*) had no stimulatory effect for the Irc3p ATPase. In contrast, the polymeric DNA cofactors (plasmid pRS316 DNA and phage M13 DNA) stimulated Irc3p ATPase activity. Remarkably, the double-stranded plasmid DNA pRS316 was significantly more efficient than M13 DNA, which is mostly single-stranded with short palindromic double-stranded regions. Finally, we tested two complementary ssDNA oligonucleotides (A and B) and the double-stranded duplex DNA (A-B) formed by annealing of the individual oligonucleotides (Figure 5D). Both single-stranded 46-mer oligonucleotides A and B had very little stimulatory effect in the Irc3p ATPase assay, whereas the A-B 46-bp duplex structure was almost as efficient a cofactor as the pRS316 plasmid DNA. We conclude that Irc3p is a dsDNA-dependent ATPase. No significant helicase activity of Irc3p was detected with a number of DNA and RNA substrates tested (Supplementary Figure S5).

Analysis of mtDNA topology reveals epistatic interactions between IRC3 and RPO41, the mitochondrial RNA polymerase

The characteristic dsDNA-dependent ATPase activity of Irc3p suggests that the protein could stimulate the remodeling of protein-DNA complexes or alternative DNA structures. In *wt rho+* mtDNA, disruption of Irc3p had prominent effects in actively transcribed regions of the mitochondrial genome, namely, in the mtDNA fragment FI containing a part of *COX2*, *tRNAMet* gene and in the mtDNA fragment FIII containing the active *ori5*. This suggested a possible link between mitochondrial transcription and the detected Irc3p-dependent changes of mtDNA topology. As the *wt rho+* genome is unstable in the absence of mitochondrial gene expression, we decided to focus on *rho−* mutants that can be maintained without mitochondrial gene expression and generated a1184 *rpo41Δ* and a1184 (*irc3Δ*, *rpo41Δ*) double-knockout strains where the mitochondrial RNA polymerase *RPO41* has been disrupted. Only a fraction of colonies obtained through the disruption of IRC3 in a1184 *rpo41Δ* contained mtDNA, but the repeat size was identical to the original a1184 mtDNA (Figure 6A and D). Disruption of *RPO41* in a1184 *irc3Δ* strain almost never produced colonies that contained the original 1.2 kb *rho−* repeat (data not shown). mtDNA in the a1184 *rpo41Δ* strain contained significantly longer dsDNA molecules (DS) and high levels of circular mtDNA forms while the unresolved heterogeneous cloud was weaker (C) compared to *wt* a1184. To confirm that the changes in

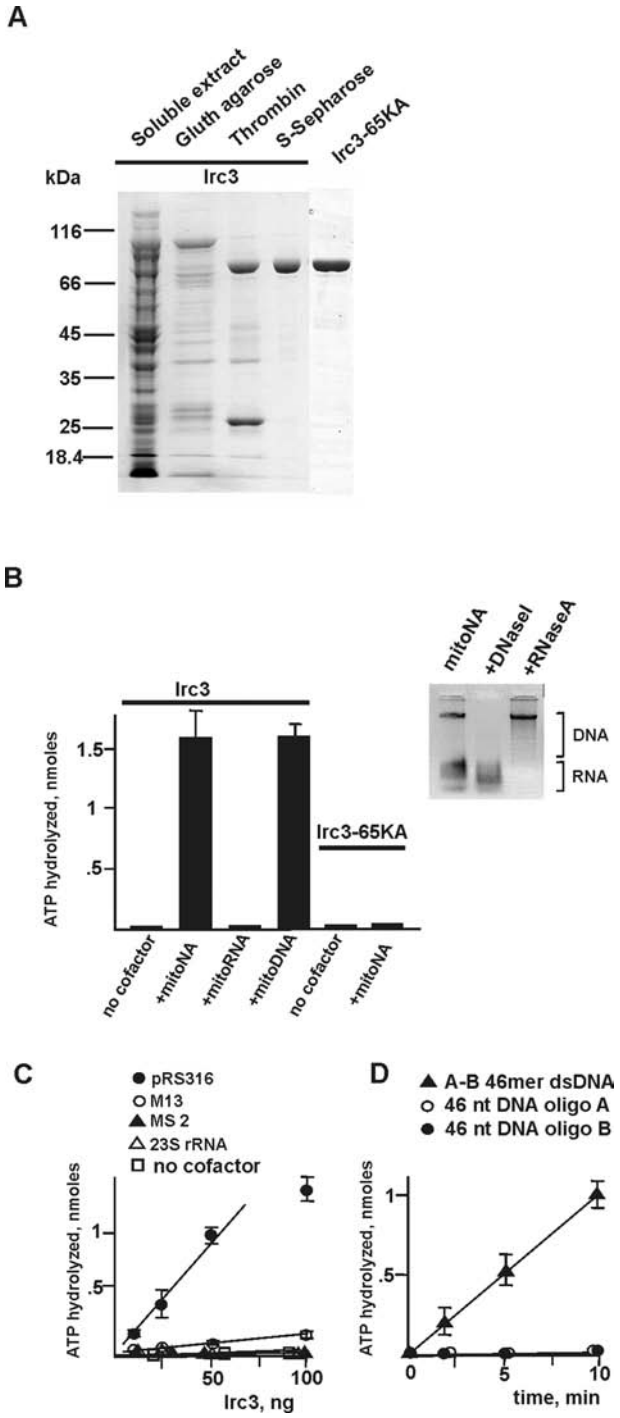

Figure 5. Analysis of enzymatic activities of Irc3p reveals the stimulatory function of dsDNA. (A) Purification of the recombinant Irc3p. Coomassie stained gel illustrating the purification steps of wt Irc3p and the purified preparation of Irc3p-65KA. (B) Stimulation of the Irc3 ATPase with total mitochondrial nucleic acid (mitoNA), mtDNA and mitochondrial RNA. The inset shows 0.5 μg of nucleic acid cofactors, prepared as described in Supplementary Material and Methods, separated on 1% agarose gel and stained with ethidium bromide. Error bars on the panel B represent the standard deviation of three independent assays. (C) Stimulation of Irc3p ATPase with different heterologous RNA and DNA cofactors. (D) Stimulation of Irc3p (25 ng/reaction) ATPase with complementary oligonucleotides A and B and with the AB dsDNA. Error bars on the panels C and D represent the standard deviation of four independent assays.

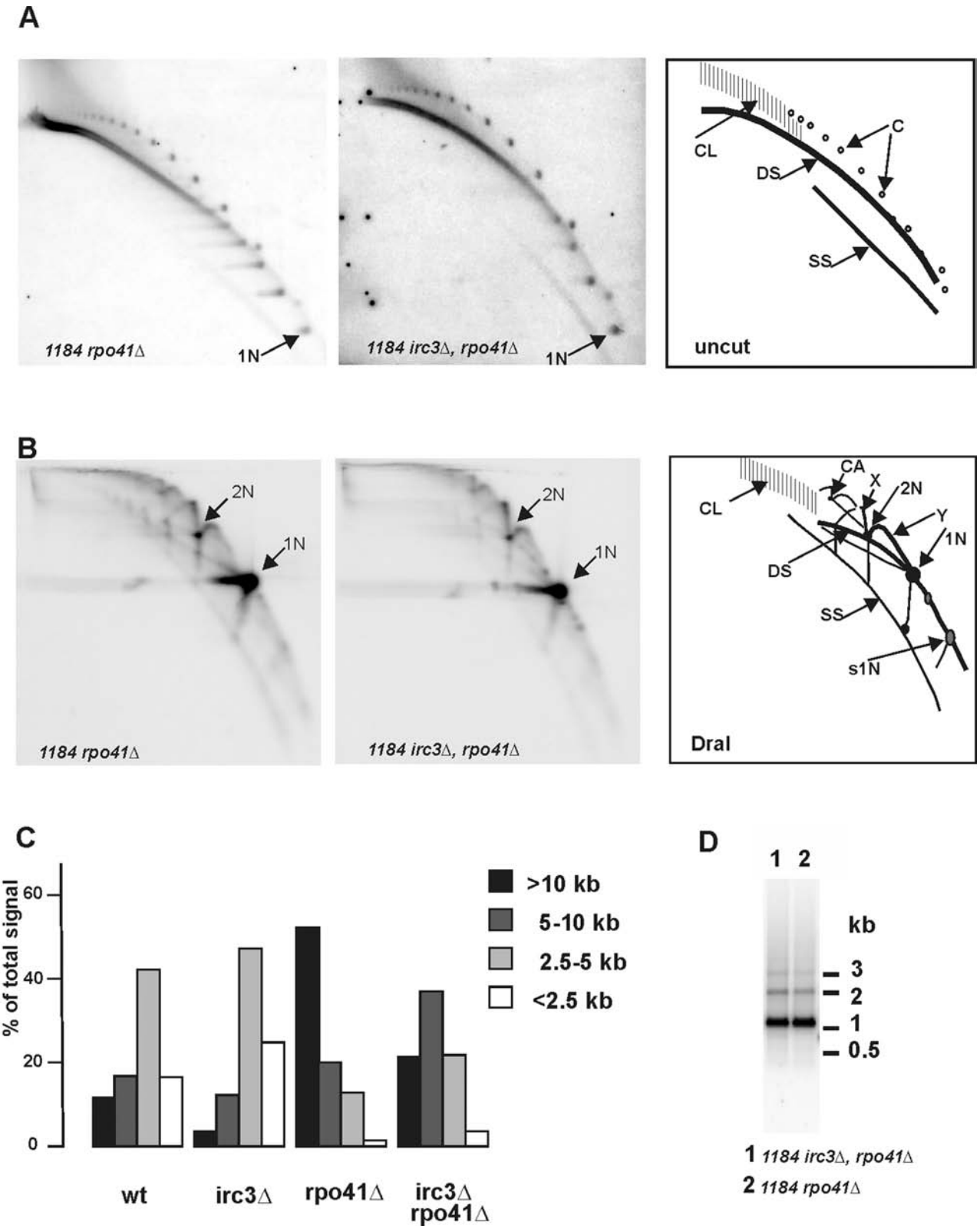

Figure 6. Disruption of the mitochondrial RNA polymerase *RPO41* restores wt mtDNA topology in the *irc3*Δ mutant. (A) 2D NAGE analysis of intact a1184 *rho*− mtDNA in *rpo41Δ* mutants. Arrows indicate the position of the 1N supercoiled circle. (B) 2D NAGE analysis of DraI digested a1184 *rho*− mtDNA in *rpo41Δ* mutants. All blots were probed with a ^{32}P labeled probe that covers the full length of the repeat. (C) Quantification of the mtDNA molecules size distributions in various strains isogenic with a1184. Shown are the relative signals corresponding to linear molecules of the indicated size. (D) 1D NAGE of DraI digested mtDNA of 1184 *rpo41Δ irc3Δ* and 1184 *rpo41Δ* strains. The blot was probed with a ^{32}P labeled probe that covers the full length of the repeat.

mtDNA topology were associated with loss of transcription, we next additionally disrupted the mitochondrial transcription factor *MTF1* in a1184. Mtfip is the mitochondrial RNA polymerase specificity factor required for promoter recognition by Rpo41p (49,50). mtDNA molecules in a1184 mtf1Δ strain were remarkably similar to those in a1184 *rpo41Δ* strain, supporting the idea that the loss of transcription is the cause of topology changes in a1184 *rpo41Δ* strain (Supplementary Figure S6). Furthermore, overexpression of Rpo41p from a multicopy plasmid has an opposite effect compared to disruption of the gene (Supplementary Figure S6). mtDNA concatemeric molecules became shorter and heterogeneous unresolved molecules formed a larger fraction than in the wt a1184 cells grown under similar conditions. All these data indicated that active mitochondrial transcription obstructs the synthesis of long concatemeric mtDNA molecules.

We next analyzed mtDNA of a1184 (*irc3Δ*, *rpo41Δ*) double-knockout strain and surprisingly found that the irc3Δ-specific changes of mtDNA topology were not present. The mtDNA metabolic intermediates in this strain were similar to the strain with *wt* nuclear background (Figure 6B, compared to Figure 4B and 4C). The intact mtDNA of a1184 (*irc3Δ*, *rpo41Δ*) contained long dsDNA (DS), circular forms of mtDNA (C) and long ssDNA intermediates, features that were not detected in mtDNA of a1184 *irc3Δ* (Figures 4C, 6A and 6C). The analysis of DraI digested mtDNA of a1184 (*irc3Δ*, *rpo41Δ*) also revealed close similarities to the topology of wt a1184 mtDNA (Figure 6B, compare to Figure 4D). The Y-arc, X-arcs and the ssDNA arc reappeared in a1184 (*irc3Δ*, *rpo41Δ*) and the dsDNA arc was weaker in a1184 (*irc3Δ*, *rpo41Δ*) compared to a1184 *irc3Δ*. Importantly, the sub-1N spots s1-s3 characteristic of a1184 *irc3Δ* were not detected in a1184 (*irc3Δ*, *rpo41Δ*). Thus, the function of Irc3 appears to be less important in the absence of mitochondrial transcription. However, Irc3p must also have a role that is independent of Rpo41 and mitochondrial transcription as the disruption of *IRC3* reduced the length of concatemeric mtDNA molecules in 1184 *rpo41*Δ strain (Figure 6A and C).

DISCUSSION

IRC3 gene was first identified in a large-scale screen for yeast mutants that have elevated levels of Rad52 foci in the cell nucleus. Here, we demonstrate that Irc3p is a dsDNA-dependent ATPase, involved directly in mtDNA metabolism. Our data suggest that Irc3p is required to avoid the accumulation of dsDNA breaks that could irreversibly damage the mitochondrial genetic system. It is likely that the instability of the mitochondrial genome in *irc3Δ* mutant strain leads to defects in iron-sulfur cluster assembly and to elevated levels of reactive oxygen species (ROS), both factors contributing to the damage of the nuclear DNA and eventual accumulation of Rad52 foci that was the basis of the IRC screen (20). Several other mitochondrial proteins were identified in the original IRC screen and it would be interesting to analyze the stability of *rho+* mitochondrial genome in the corresponding mutants.

In silico analysis indicates that Irc3p belongs to the SFII of helicases and nucleic acid-dependent ATPases. SFII is a large group of proteins with diverse biochemical functions, including RNA and DNA helicases and ATPases that remodel protein-DNA complexes or translocate along double-stranded nucleic acids without unwinding their substrate. SFII RNA helicases Mhr4p, Mss116p and Suv3p have previously been characterized in yeast mitochondria (25,26,28,31,34,39). Irc3p is annotated as a putative RNA helicase in different databases, however, no supporting experimental evidence has been published. Our analysis indicates that the ATPase activity of Irc3p is stimulated by dsDNA and the protein has a specific role in mtDNA metabolism contradicting the current annotation. Differences of biochemical properties between the yeast mitochondrial SFII enzymes are revealed in simple phenotypic tests of mutant strains. Disruption of *MHR4*, *MSS116* or *SUV3* rapidly inactivates mitochondrial gene expression. This, in turn, leads to a loss of the functional *rho+* mitochondrial genome in the mutant yeast cells, rendering them unviable on a non-fermentable carbon source. In contrast, the kinetics of *rho+* mtDNA loss is relatively slow in *irc3Δ* cells. Previously, similar slow mtDNA loss phenotype has been described for mutants of the mtDNA packaging protein Abf2p. *abf2Δ* mutants lose the functional mitochondrial genome, unless the cells are grown on a non-fermentable carbon source, and interestingly, *rho−* *abf2Δ* mutants have a distinctive recombination phenotype (51,52). Our data indicate that the loss of respiratory competence of irc3Δ yeast cells is accompanied with accumulation of dsDNA breaks in mitochondria. We cannot rule out a possibility that in *rho+* cells the defects of mtDNA are generated indirectly by a mechanism that involves impaired gene expression in the irc3Δ mutants. However, similar breaks of mtDNA are generated also in *rho−* strains. Mitochondrial ribosomes and tRNAs are not synthesized in the mitochondria of *rho−* yeast strains and consequently the changes of mitochondrial gene expression cannot influence mtDNA metabolism. Therefore, we suggest that the loss of Irc3p function and the accumulation of double-stranded ends or breaks in mtDNA are directly linked. Furthermore, we found that the double-stranded breaks in the mtDNA of irc3Δ yeast mutants are not randomly distributed, but map to GC-rich blocks, both in the wt *rho+* and the mutant *rho−* mitochondrial genomes. At least some dsDNA breaks of *rho+* mtDNA appear at the same positions in the *rho−* strain, including the breaks in the C-box and the AB palindrome of the active *ori* (compare Figure 3D, FIII, and Figure 4D), supporting a common formation mechanism. Genetic experiments have previously revealed that the GC-rich elements in yeast mtDNA represent recombination hotspots (53,54). Double-stranded breaks can be generated at these sequences spontaneously during regular mtDNA metabolism or are induced by physical effectors or by specific mutant background (55). Recently, it has been demonstrated that artificially induced dsDNA breaks can be tolerated by the yeast mitochondrial genetic system (56). We suggest that double-stranded breaks could be a part of regular mtDNA replication initiation pathway in yeast mitochondria and propose that Irc3p is player that regulates the level of these double-stranded breaks or free ends of DNA.

Why do the dsDNA breaks accumulate in *irc3*Δ mutants? The steady-state level of double-stranded breaks depends

on the rate of their formation and removal. First, Irc3p could stimulate the removal of dsDNA breaks by a mechanism that involves homologous recombination. Distinctive changes in *rho*− mtDNA metabolic intermediates that can be detected in the *irc3*Δ mutant suggest that a specific recombination pathway is affected (Figure 4D). The X-arc is composed of four-way branched DNA structures that most likely represent recombination intermediates (57). Formation of circular mtDNA molecules from the concatemeric linear DNA has also been proposed to be a recombination-based process (10). Both the circular forms and the X-arc are diminished in the *irc3Δ rho*-yeast strain. We also note that the fraction of heterogeneous mtDNA molecules (CL-cloud) is more prominent in the *irc3Δ* mutant than in the *wt rho*− strain. These complex intermediates are S1 nuclease sensitive (not shown), contain extensive single-stranded regions and are therefore probably formed by a single-strand annealing mechanisms, which could drive the synthesis of mtDNA in the *irc3*Δ mutant strain. In conclusion, the changes of *rho*− mtDNA topology in the *irc3Δ* strain suggest that Irc3p could stimulate recombinative repair of double-stranded breaks in yeast mitochondria.

Several potential components of the enzymatic machinery involved in mitochondrial recombination have been identified, including the MRX complex (56), the homolog of Rad52p, Mgm101p (15,58); Mhr1p that has a function in gene conversion (16,46) and two helicases Hmi1p and Pif1p (59,60). In this context, Irc3p as a dsDNA-dependent ATPase could potentially fulfill the functions of nuclear dsDNA translocase Rad54p, which plays multiple roles in Rad51p-dependent D-loop formation events (61).

It is likely that Irc3p stimulates dsDNA repair via recombinational pathway, but currently we cannot rule out, that Irc3p activity inhibits the formation of the dsDNA breaks. While several factors can contribute to the formation of these structures in mitochondria, our analysis of the topology of *rho*− mtDNA underlines the role of transcription in this process. In the yeast mitochondrial genome, specific transcription of *ori* elements is thought to be required for transcription-primed DNA synthesis. Transcription is not essential for the stability of *rho*− mtDNA, as *rpo41* disruption mutants support the replication of rho− genomes (62,63). Paradoxically, a prominent class of *rho*− mitochondrial genomes contains specific transcription-associated *cis*-elements known as *ori* or *rep* (64,65). Active *ori* elements are present also in *rho*− genomes analyzed in the current study. Our data confirm the previous findings that *rho*− genomes do not require transcription for stability. However, we find that intact mtDNA concatemers are significantly longer in *rpo41Δ* strains compared to the strains that contain Rpo41p, indicating that transcription could stimulate the formation of dsDNA breaks (Figure 6C). Active *ori* elements contain a non-anucleotide promoter for the mitochondrial RNA polymerase Rpo41p and three G/C-rich boxes A, B and C (11). According to a previously proposed model, transcription at active *ori* elements generates an R-loop that is used to prime DNA at the conserved C box and this could create a free DNA end at the *ori* C element. Alternatively, the R loops themselves could represent obstacles for the mtDNA polymerase. DNA double-stranded breaks in mitochondria could also form as a result of direct collisions between transcription and replication machineries as described in a variety of prokaryotic and eukaryotic systems (66). In higher eukaryotes, a specific mechanism used to minimize replication and transcription encounters in mitochondria of multicellular organisms is thought to depend on a specific family of transcription termination factors or TERFs (67). However, yeast mitochondria do not have TERF family proteins leaving open the possibility that different mechanisms could exist to overcome the potential damage resulting from conflicts between replication and transcription machineries (15,16,46,56,58–61).

Finally, Irc3p is not conserved in mammalian mitochondria, however, recent reports have indicated that a Swi/Snf family member, CSB (Cockayne Syndrome group B) protein, has a mitochondrial function (68–71). These findings and our data presented in the current study raise a possibility that dsDNA-dependent ATPase-driven translocase activity is universally required in mtDNA metabolism.

SUPPLEMENTARY DATA

Supplementary Data are available at NAR Online.

ACKNOWLEDGEMENTS

We thank A. Abroi, I. Ilves and L. Sedman for helpful comments on the manuscript. We thank R. Stuart and W. Neupert for antibodies against specific mitochondrial proteins and M. Leppik for MS2 and 23S RNA. We thank M. Loorits for technical assistance and D. Lubenets with T. Tamm for performing preliminary experiments of Irc3-GFP localization.

FUNDING

Estonian Science Foundation [8449 to T.S.; 8845 to J.S.]; Estonian Institutional Funding Grant from Estonian Research Council [IUT14021]. Funding for open access charge: Estonian Institutional Funding Grant from Estonian Research Council [IUT14021].
Conflict of interest statement. None declared.

REFERENCES

1. Schmidt,O., Pfanner,N. and Meisinger,C. (2010) Mitochondrial protein import: from proteomics to functional mechanisms. *Nat. Rev. Mol. Cell Biol.*, **11**, 655–667.
2. Foury,F., Roganti,T., Lecrenier,N. and Purnelle,B. (1998) The complete sequence of the mitochondrial genome of *Saccharomyces cerevisiae*. *FEBS Lett.*, **440**, 325–331.
3. Nunnari,J. and Suomalainen,A. (2012) Mitochondria: in sickness and in health. *Cell*, **148**, 1145–1159.
4. Park,C.B. and Larsson,N. (2011) Mitochondrial DNA mutations in disease and aging. *J. Cell Biol.*, **193**, 809–818.
5. Taylor,R.W. and Turnbull,D.M. (2005) Mitochondrial DNA mutations in human disease. *Nat. Rev. Genet.*, **6**, 389–402.
6. Foury,F. (1989) Cloning and sequencing of the nuclear gene MIP1 encoding the catalytic subunit of the yeast mitochondrial DNA polymerase. *J. Biol. Chem.*, **264**, 20552–20560.
7. Contamine,V. and Picard,M. (2000) Maintenance and integrity of the mitochondrial genome: a plethora of nuclear genes in the budding yeast. *Microbiol. Mol. Biol. Rev.*, **64**, 281–315.
8. Dujon,B. (1981) Mitochondrial genes and function. In: Broach,J., Jones,E. and Strathern,J. (eds.). *The Molecular Biology of the Yeast Saccharomyces*. Cold Spring Harbor Laboratory, Cold Spring Harbor, N.Y., pp. 505–635.

9. Lecrenier,N. and Foury,F. (2000) New features of mitochondrial DNA replication system in yeast and man. *Gene*, **246**, 37–48.
10. MacAlpine,D.M., Kolesar,J., Okamoto,K., Butow,R.A. and Perlman,P.S. (2001) Replication and preferential inheritance of hypersuppressive petite mitochondrial DNA. *EMBO J.*, **20**, 1807–1817.
11. Baldacci,G. and Bernardi,G. (1982) Replication origins are associated with transcription initiation sequences in the mitochondrial genome of yeast. *EMBO J.*, **1**, 987–994.
12. Baldacci,G., Cherifzahar,B. and Bernardi,G. (1984) The initiation of DNA replication in the mitochondrial genome of yeast. *EMBO J.*, **3**, 2115–2120.
13. Graves,T., Dante,M., Eisenhour,L. and Christianson,T.W. (1998) Precise mapping and characterization of the RNA primers of DNA replication for a yeast hypersuppressive petite by in vitro capping with guanylyltransferase. *Nucleic Acids Res.*, **26**, 1309–1316.
14. Sedman,T., Kuusk,S., Kivi,S. and Sedman,J. (2000) A DNA helicase required for maintenance of the functional mitochondrial genome in *Saccharomyces cerevisiae*. *Mol. Cell. Biol.*, **20**, 1816–1824.
15. Chen,X.J., Guan,M.X. and Clark-Walker,G.D. (1993) MGM101, a nuclear gene involved in maintenance of the mitochondrial genome in *Saccharomyces cerevisiae*. *Nucleic Acids Res.*, **21**, 3473–3477.
16. Ling,F., Makishima,F., Morishima,N. and Shibata,T. (1995) A nuclear mutation defective in mitochondrial recombination in yeast. *EMBO J.*, **14**, 4090–4101.
17. Myers,A.M., Pape,L.K. and Tzagoloff,A. (1985) Mitochondrial protein-synthesis is required for maintenance of intact mitochondrial genomes in *Saccharomyces cerevisiae*. *EMBO J.*, **4**, 2087–2092.
18. Dickinson,B.C. and Chang,C.J. (2011) Chemistry and biology of reactive oxygen species in signaling or stress responses. *Nat. Chem. Biol.*, **7**, 504–511.
19. Veatch,J.R., McMurray,M.A., Nelson,Z.W. and Gottschling,D.E. (2009) Mitochondrial dysfunction leads to nuclear genome instability via an iron-sulfur cluster defect. *Cell*, **137**, 1247–1258.
20. Alvaro,D., Lisby,M. and Rothstein,R. (2007) Genome-wide analysis of Rad52 foci reveals diverse mechanisms impacting recombination. *PloS Genet.*, **3**, 2439–2449.
21. Huh,W.K., Falvo,J.V., Gerke,L.C., Carroll,A.S., Howson,R.W., Weissman,J.S. and O'Shea,E.K. (2003) Global analysis of protein localization in budding yeast. *Nature*, **425**, 686–691.
22. Byrd,A.K. and Raney,K.D. (2012) Superfamily 2 helicases. *Frontiers Biosci.-Landmark*, **17**, 2070–2088.
23. Gorbalenya,A.E., Koonin,E.V., Donchenko,A.P. and Blinov,V.M. (1989) 2 related superfamilies of putative helicases involved in replication, recombination, repair and expression of DNA and RNA genomes. *Nucleic Acids Res.*, **17**, 4713–4730.
24. de la Cruz,J., Kressler,D. and Linder,P. (1999) Unwinding RNA in *Saccharomyces cerevisiae*: DEAD-box proteins and related families. *Trends Biochem. Sci.*, **24**, 192–198.
25. Seraphin,B., Simon,M., Boulet,A. and Faye,G. (1989) Mitochondrial splicing requires a protein from a novel helicase family. *Nature*, **337**, 84–87.
26. Huang,H.R., Rowe,C.E., Mohr,S., Jiang,Y., Lambowitz,A.M. and Perlman,P.S. (2005) The splicing of yeast mitochondrial group I and group II introns requires a DEAD-box protein with RNA chaperone function. *Proc. Natl. Acad. Sci. U.S.A.*, **102**, 163–168.
27. Solem,A., Zingler,N. and Pyle,A.M. (2006) A DEAD protein that activates intron self-splicing without unwinding RNA. *Mol. Cell*, **24**, 611–617.
28. Halls,C., Mohr,S., Del Campo,M., Yang,Q., Jankowsky,E. and Lambowitz,A.M. (2007) Involvement of DEAD-box proteins in group I and group II intron splicing. biochemical characterization of Mss116p, ATP hydrolysis-dependent and -independent mechanisms, and general RNA chaperone activity. *J. Mol. Biol.*, **365**, 835–855.
29. Del Campo,M., Tijerina,P., Bhaskaran,H., Mohr,S., Yang,Q., Jankowsky,E., Russell,R. and Lambowitz,A.M. (2007) Do DEAD-box proteins promote group II intron splicing without unwinding RNA? *Mol. Cell*, **28**, 159–166.
30. Stepien,P.P., Margossian,S.P., Landsman,D. and Butow,R.A. (1992) The yeast nuclear gene Suv3 affecting mitochondrial posttranscriptional processes encodes a putative ATP-dependent RNA helicase. *Proc. Natl. Acad. Sci. U.S.A.*, **89**, 6813–6817.
31. Dziembowski,A., Piwowarski,J., Hoser,R., Minczuk,M., Dmochowska,A., Siep,M., van der Spek,H., Grivell,L. and Stepien,P.P. (2003) The yeast mitochondrial degradosome - its composition, interplay between RNA helicase and RNase activities and the role in mitochondrial RNA metabolism. *J. Biol. Chem.*, **278**, 1603–1611.
32. Golik,P., Szczepanek,T., Bartnik,E., Stepien,P.P. and Lazowska,J. (1995) The *Saccharomyces cerevisiae* nuclear gene Suv3 encoding a putative RNA helicase is necessary for the stability of mitochondrial transcripts containing multiple introns. *Curr. Genet.*, **28**, 217–224.
33. Guo,X.E., Chen,C., Wang,D.D., Modrek,A.S., Hoai Phan,Vy, Lee,W. and Chen,P. (2011) Uncoupling the roles of the SUV3 helicase in maintenance of mitochondrial genome stability and RNA degradation. *J. Biol. Chem.*, **286**, 38783–38794.
34. De Silva,D., Fontanesi,F. and Barrientos,A. (2013) The DEAD box protein Mrh4 functions in the assembly of the mitochondrial large ribosomal subunit. *Cell Metab.*, **18**, 712–725.
35. Schmidt,U., Lehmann,K. and Stahl,U. (2002) A novel mitochondrial DEAD box protein (Mrh4) required for maintenance of mtDNA in *Saccharomyces cerevisiae*. *Fems Yeast Res.*, **2**, 267–276.
36. Sherman,F. (1991) Getting started with yeast. *Meth. Enzymol.*, **194**, 3–21.
37. Kuusk,S., Sedman,T., Joers,P. and Sedman,J. (2005) Hmi1p from *Saccharomyces cerevisiae* mitochondria is a structure-specific DNA helicase. *J. Biol. Chem.*, **280**, 24322–24329.
38. Gerhold,J.M., Aun,A., Sedman,T., Joers,P. and Sedman,J. (2010) Strand invasion structures in the inverted repeat of *Candidaalbicans* mitochondrial DNA reveal a role for homologous recombination in replication. *Mol. Cell*, **39**, 851–861.
39. Turk,E.M. and Caprara,M.G. (2010) Splicing of yeast aI5 beta group I intron requires SUV3 to recycle MRS1 via mitochondrial degradosome-promoted decay of excised intron ribonucleoprotein (RNP). *J. Biol. Chem.*, **285**, 8585–8594.
40. Bifano,A.L., Turk,E.M. and Caprara,M.G. (2010) Structure-guided mutational analysis of a yeast DEAD-box protein involved in mitochondrial RNA splicing. *J. Mol. Biol.*, **398**, 429–443.
41. Voegtle,F.-., Wortelkamp,S., Zahedi,R.P., Becker,D., Leidhold,C., Gevaert,K., Kellermann,J., Voos,W., Sickmann,A., Pfanner,N. *et al.* (2009) Global analysis of the mitochondrial N-proteome identifies a processing peptidase critical for protein stability. *Cell*, **139**, 428–439.
42. Linder,P. and Jankowsky,E. (2011) From unwinding to clamping - the DEAD box RNA helicase family. *Nat. Rev. Mol. Cell Biol.*, **12**, 505–516.
43. Schneider,S. and Schwer,B. (2001) Functional domains of the yeast splicing factor Prp22p. *J. Biol. Chem.*, **276**, 21184–21191.
44. Turk,E.M., Das,V., Seibert,R.D. and Andrulis,E.D. (2013) The mitochondrial RNA landscape of *Saccharomyces cerevisiae*. *PloS ONE*, **8**, e78105.
45. Maleszka,R., Skelly,P.J. and Clarkwalker,G.D. (1991) Rolling circle replication of DNA in yeast mitochondria. *EMBO J.*, **10**, 3923–3929.
46. Ling,F. and Shibata,T. (2004) Mhr1p-dependent concatemeric mitochondrial DNA formation for generating yeast mitochondrial homoplasmic cells. *Mol. Biol. Cell*, **15**, 310–322.
47. MacAlpine,D.M., Perlman,P.S. and Butow,R.A. (2000) The numbers of individual mitochondrial DNA molecules and mitochondrial DNA nucleoids in yeast are co-regulated by the general amino acid control pathway. *EMBO J.*, **19**, 767–775.
48. Cordin,O., Banroques,J., Tanner,N.K. and Linder,P. (2006) The DEAD-box protein family of RNA helicases. *Gene*, **367**, 17–37.
49. Lisowsky,T. and Michaelis,G. (1989) Mutations in the genes for mitochondrial RNA polymerase and a 2nd mitochondrial transcription factor of *Saccharomyces cerevisiae*. *Mol. Gen. Genet.*, **219**, 125–128.
50. Schinkel,A.H., Koerkamp,M.J.A.G. and Tabak,H.F. (1988) Mitochondrial RNA polymerase of *Saccharomyces cerevisiae* - composition and mechanism of promoter recognition. *EMBO J.*, **7**, 3255–3262.
51. Diffley,J.F.X. and Stillman,B. (1991) A close relative of the nuclear, chromosomal high-mobility group protein Hmg1 in yeast mitochondria. *Proc. Natl. Acad. Sci. U.S.A.*, **88**, 7864–7868.
52. MacAlpine,D.M., Perlman,P.S. and Butow,R.A. (1998) The high mobility group protein Abf2p influences the level of yeast mitochondrial DNA recombination intermediates in vivo. *Proc. Natl. Acad. Sci. U.S.A.*, **95**, 6739–6743.

53. Dieckmann,C.L. and Gandy,B. (1987) Preferential recombination between GC clusters in yeast mitochondrial DNA. *EMBO J.*, **6**, 4197–4203.
54. Weiller,G.F., Bruckner,H., Kim,S.H., Pratje,E. and Schweyen,R.J. (1991) A GC cluster repeat is a hotspot for mit- macro-deletions in yeast mitochondrial DNA. *Mol. Gen. Genet.*, **226**, 233–240.
55. Zinn,A.R., Pohlman,J.K., Perlman,P.S. and Butow,R.A. (1988) In vivo double-strand breaks occur at recombinogenic G + C-rich sequences in the yeast mitochondrial genome. *Proc. Natl. Acad. Sci. U.S.A.*, **85**, 2686–2690.
56. Kalifa,L., Quintana,D.F., Schiraldi,L.K., Phadnis,N., Coles,G.L., Sia,R.A. and Sia,E.A. (2012) Mitochondrial genome maintenance: roles for nuclear nonhomologous end-joining proteins in *Saccharomyces cerevisiae*. *Genetics*, **190**, 951–964.
57. Lockshon,D., Zweifel,S.G., Freemancook,L.L., Lorimer,H.E., Brewer,B.J. and Fangman,W.L. (1995) A role for recombination junctions in the segregation of mitochondrial DNA in yeast. *Cell*, **81**, 947–955.
58. Mbantenkhu,M., Wang,X., Nardozzi,J.D., Wilkens,S., Hoffman,E., Patel,A., Cosgrove,M.S. and Chen,X.J. (2011) Mgm101 is a Rad52-related protein required for mitochondrial DNA recombination. *J. Biol. Chem.*, **286**, 42360–42370.
59. Foury,F. and Kolodynski,J. (1983) Pif mutation blocks recombination between mitochondrial *rho+* and *rho-* genomes having tandemly arrayed repeat units in *Saccharomyces cerevisiae*. *Proc. Natl. Acad. Sci. U.S.A.*, **80**, 5345–5349.
60. Sedman,T., Joers,P., Kuusk,S. and Sedman,J. (2005) Helicase Hmi1 stimulates the synthesis of concatemeric mitochondrial DNA molecules in yeast *Saccharomyces cerevisiae*. *Curr. Genet.*, **47**, 213–222.
61. Wright,W.D. and Heyer,W. (2014) Rad54 functions as a heteroduplex DNA pump modulated by its DNA substrates and Rad51 during D loop formation. *Mol. Cell*, **53**, 420–432.
62. Fangman,W.L., Henly,J.W. and Brewer,B.J. (1990) Rpo41-independent maintenance of [*rho-*] mitochondrial DNA in *Saccharomyces cerevisiae*. *Mol. Cell. Biol.*, **10**, 10–15.
63. Lorimer,H.E., Brewer,B.J. and Fangman,W.L. (1995) A test of the transcription model for biased inheritance of yeast mitochondrial DNA. *Mol. Cell. Biol.*, **15**, 4803–4809.
64. Blanc,H. and Dujon,B. (1980) Replicator regions of the yeast mitochondrial DNA responsible for suppressiveness. *Proc. Natl. Acad. Sci. U.S.A.*, **77**, 3942–3946.
65. Dezamaroczy,M., Marotta,R., Faugeronfonty,G., Goursot,R., Mangin,M., Baldacci,G. and Bernardi,G. (1981) The origins of replication of the yeast mitochondrial genome and the phenomenon of suppressivity. *Nature*, **292**, 75–78.
66. Helmrich,A., Ballarino,M., Nudler,E. and Tora,L. (2013) Transcription-replication encounters, consequences and genomic instability. *Nat. Struct. Mol. Biol.*, **20**, 412–418.
67. Joers,P. and Jacobs,H.T. (2013) Analysis of replication intermediates indicates that *Drosophila melanogaster* mitochondrial DNA replicates by a strand-coupled theta mechanism. *PloS ONE*, **8**, e53249.
68. Aamann,M.D., Sorensen,M.M., Hvitby,C., Berquist,B.R., Muftuoglu,M., Tian,J., de Souza-Pinto,N.C., Scheibye-Knudsen,M., Wilson,D.M. III, Stevnsner,T. *et al.* (2010) Cockayne syndrome group B protein promotes mitochondrial DNA stability by supporting the DNA repair association with the mitochondrial membrane. *FASEB J.*, **24**, 2334–2346.
69. Berquist,B.R., Canugovi,C., Sykora,P., Wilson,D.M. III and Bohr,V.A. (2012) Human cockayne syndrome B protein reciprocally communicates with mitochondrial proteins and promotes transcriptional elongation. *Nucleic Acids Res.*, **40**, 8392–8405.
70. Kamenisch,Y., Fousteri,M., Knoch,J., von Thaler,A., Fehrenbacher,B., Kato,H., Becker,T., Dolle,M.E.T., Kuiper,R., Majora,M. *et al.* (2010) Proteins of nucleotide and base excision repair pathways interact in mitochondria to protect from loss of subcutaneous fat, a hallmark of aging. *J. Exp. Med.*, **207**, 379–390.
71. Osenbroch,P.O., Auk-Emblem,P., Halsne,R., Strand,J., Forstrom,R.J., van der Pluijm,I. and Eide,L. (2009) Accumulation of mitochondrial DNA damage and bioenergetic dysfunction in CSB defective cells. *FEBS J.*, **276**, 2811–2821.